Tellus (2006), 58B, 560–572
Printed in Singapore. All rights reserved

TELLUS

Nitrogen fixation amplifies the ocean biogeochemical response to decadal timescale variations in mineral dust deposition

By J. KEITH MOORE[1]*, SCOTT C. DONEY[2], KEITH LINDSAY[3], NATALIE MAHOWALD[3] and ANTHONY F. MICHAELS[4], [1]*University of California, Irvine, Department of Earth System Science, Irvine, CA 92697-3100, U.S.A.;* [2]*Woods Hole Oceanograhic Institution, Department of Marine Chemistry and Geochemistry, MS #25, Woods Hole, MA 02543-1543, U.S.A.;* [3]*National Center for Atmospheric Research, P.O. Box 3000, Boulder, CO 80307-3000, U.S.A.;* [4]*University of Southern California, Biology Department, Los Angeles, CA, 90089-0371, U.S.A.*

(Manuscript received 30 November 2005; in final form 26 June 2006)

ABSTRACT

A global ocean biogeochemical model is used to quantify the sensitivity of marine biogeochemistry and air–sea CO_2 exchange to variations in dust deposition over decadal timescales. Estimates of dust deposition generated under four climate states provide a large range in total deposition with spatially realistic patterns; transient ocean model experiments are conducted by applying a step-function change in deposition from a current climate control. Relative to current conditions, higher dust deposition increases diatom and export production, nitrogen fixation and oceanic net CO_2 uptake from the atmosphere, while reduced dust deposition has the opposite effects. Over timescales less than a decade, dust modulation of marine productivity and export is dominated by direct effects in high-nutrient, low-chlorophyll regions, where iron is the primary limiting nutrient. On longer timescales, an indirect nitrogen fixation pathway has increased importance, significantly amplifying the ocean biogeochemical response. Because dust iron input decouples carbon cycling from subsurface macronutrient supply, the ratio of the change in net ocean CO_2 uptake to change in export flux is large, 0.45–0.6. Decreasing dust deposition and reduced oceanic CO_2 uptake over the next century could provide a positive feedback to global warming, distinct from feedbacks associated with changes in stratification and circulation.

1. Introduction

Climate-induced variations in atmospheric dust deposition can significantly impact the marine carbon cycle because biological production and export are iron limited in many regions. Mineral dust deposition is the main external source to the oceans of the critical micro-nutrient iron, which limits phytoplankton growth rates over some 30–40% of the oceans in the high-nitrate, low-chlorophyll (HNLC) regions (Martin et al., 1991; Fung et al., 2000; Moore et al., 2004; Jickells et al., 2005; Mahowald et al., 2005). The HNLC regions, concentrated in the sub-Arctic North Pacific, the equatorial Pacific and in the Southern Ocean, are areas of low dust deposition (Fig. 1), where primary production, export production and air–sea CO_2 exchange should respond directly to variations in iron inputs from the atmosphere.

*Corresponding author.
e-mail: jkmoore@uci.edu
DOI: 10.1111/j.1600-0889.2006.00209.x

Mesoscale in situ iron fertilization experiments have demonstrated the strong control of surface iron concentrations in HNLC regions. A typical response to iron additions involves a shift in the phytoplankton community composition from smaller cells to larger cells (typically diatoms), large increases in biomass and primary production, and large decreases in surface water macronutrient concentrations and pCO_2 values (Coale et al., 1996; Boyd et al., 2000; Tsuda et al., 2003; Coale et al., 2004; de Baar et al., 2005). In subtropical and tropical regions, where nitrogen is typically the growth-limiting nutrient for the phytoplankton community, the nitrogen-fixing diazotrophs may be limited by iron and, thus, sensitive to dust inputs (Falkowski, 1997; Berman-Frank et al. 2001; Michaels et al., 2001; Kustka et al., 2002; Moore et al., 2004). The diazotrophs are able to obtain N from dissolved N_2 gas and require more iron than other phytoplankton (Berman-Frank et al., 2001; Kustka et al., 2003). *Trichodesmium*, the most common diazotroph, accounts for little export directly; however, their release of new bioavailable nitrogen through excretion and mortality

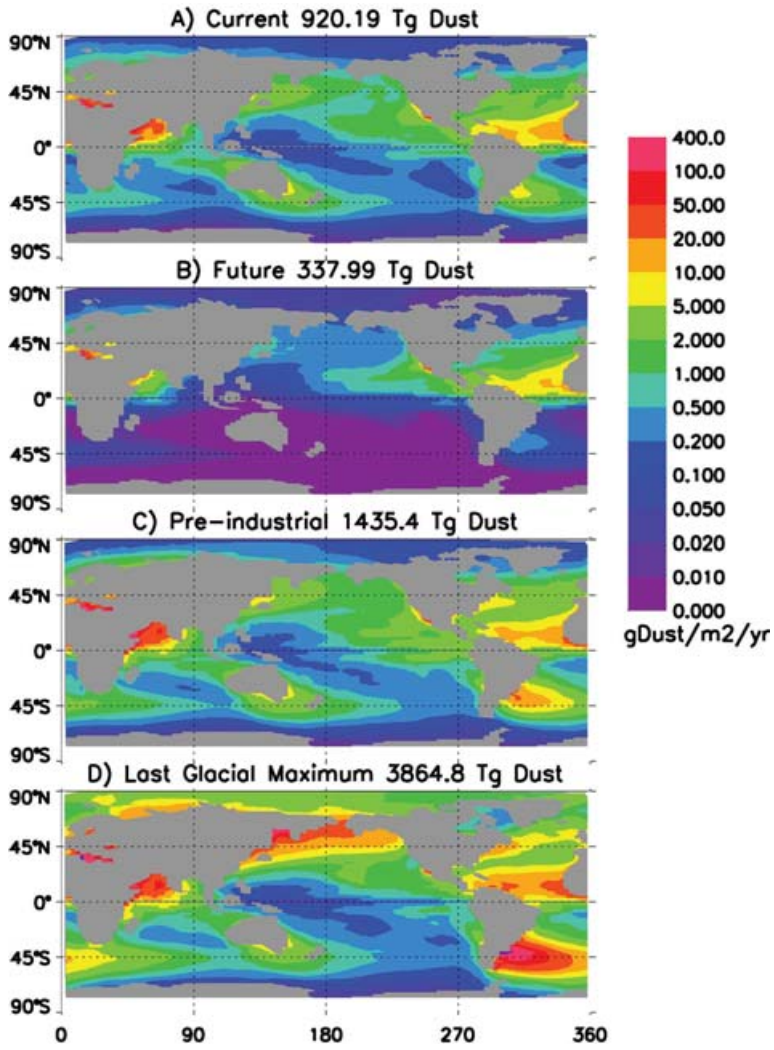

Fig. 1. Total dust deposition to the oceans estimated for different climate regimes (Current, Future, Pre-industrial, Last Glacial Maximum) are depicted.

(Glibert and Bronk, 1994; Mahaffey et al., 2005) enhances primary and export production by the rest of the phytoplankton community. A number of previous studies have discussed the potential climate feedbacks involving dust deposition, nitrogen fixation, the strength of the biological pump and air–sea exchange of CO_2 (Falkowski, 1997; Michaels et al., 2001; Karl et al., 2002; Gruber, 2004; Moore et al., 2004; Jickells et al., 2005). We refer to this dust-nitrogen fixation-carbon linkage as the indirect pathway for dust deposition to influence air–sea CO_2 exchange.

In this study a Biogeochemical Elemental Cycling (BEC) ocean model (Moore et al., 2004) is used to examine the sensitivity of ocean biogeochemistry and air–sea CO_2 exchange to climate-driven changes in mineral dust deposition to the oceans. New estimates of dust deposition generated under four climate regimes (Current era, Pre-industrial era, a Future climate with atmospheric CO_2 concentrations at double pre-industrial levels, and the climate of the Last Glacial Maximum, LGM) are used to drive the BEC ocean model. Transient multidecade experiments are conducted where the oceanic dust inputs are altered as a step-function from Current era conditions. In earlier work, we examined ecological responses to an arbitrary doubling or halving of dust deposition (Moore et al., 2002b, 2004). These new dust simulations provide a wide range of dust deposition levels that can be used to examine ocean biogeochemical sensitivity, while retaining realistic spatial distributions consistent with their respective climate states (Mahowald et al., 2006). Further in contrast with our earlier studies, by explicitly incorporating the inorganic CO_2 system into our model, we explore here the impact of altered dust on both biological dynamics and air–sea CO_2 exchange. Our goal is not to simulate ocean biogeochemical cycling under these various climate regimes, but only to examine the sensitivity to plausible climate-driven variations in dust deposition. Future work will involve coupled dust-carbon cycle-climate forcing of the ocean (Fung et al., 2005; Doney et al., 2006).

2. Methods

Mineral dust deposition to the oceans is estimated under four climate regimes: Current era, Pre-industrial era, Future climate scenario with atmospheric CO_2 concentrations at double pre-industrial levels, and the climate of the LGM. Terrestrial dust sources, entrainment, atmospheric transport and ocean deposition are calculated within equilibrium climate simulations using the National Center for Atmospheric Research (NCAR) Community Climate System Model (CCSM3) using a slab ocean model; a complete model description, and comparison to observations for these cases is included in Mahowald et al. (2006), so that we include only a brief description here. Dust sources and deposition are calculated following the Dust Entrainment And Deposition (DEAD) module, which includes four dust size bins with a log normal distribution within each size bin (Zender et al., 2003). We used a larger source sub-bin size distribution of 3.5 μm median diameter instead of 2.54 μm to better match observations (Grini and Zender, 2004). Transport and deposition are calculated within the climate model, with wet deposition based on Rasch et al. (2001) and dry deposition following Zender et al. (2003a). Simulations are conducted in the slab ocean model version of the Community Atmosphere Model component (Kiehl et al., 2006; Otto-Bliesner et al., 2006). Dust sources are calculated using the 'geomorphic' based soil erodibility factor from Zender et al. (2003b). For this set of simulations, we include changes in vegetation using the equilibrium vegetation model BIOME 3 (Haxeltine and Prentice, 1996), similar to previous studies (e.g. Mahowald et al., 1999, 2006; Werner et al., 2002; Mahowald and Luo, 2003), as well as glaciogenic sources for the LGM (Zarate, 2003). These glaciogenic sources are tuned to best match available observations for dust deposition. Vegetation distributions are a function of precipitation, temperature, cloudiness, and atmospheric CO_2 concentrations, which allows for a CO_2 fertilization effect. Only natural dust sources are included; land use sources of dust could be important on these timescales (Mahowald and Luo, 2003), but there is a large uncertainty in the magnitude of these sources in literature (e.g. Mahowald and Luo, 2003; Mahowald et al., 2004; Tegen et al., 2004;). For the LGM simulation, comparisons are made to the DIRTMAP deposition compilation (Kohfeld and Harrison, 2001) and terrestrial sediment records (Mahowald et al., 2006). Similar to Mahowald et al. (1999), in these simulations changes in the source areas are crucial for capturing the large dust deposition fluctuations seen in the high-latitude ice cores. These simulations reproduce observed dust concentration distributions and deposition distributions for the current era and for the LGM (Mahowald et al., 2006).

The BEC ocean model runs within the NCAR CCSM3 utilizing the coarse-resolution (3.6 degree in longitude; 0.9–2.0 degree in latitude, with finer resolution at the equator) Parallel Ocean Program (POP) ocean circulation component (Collins et al., 2006; Yeager et al., 2006). The model includes multiple potentially growth-limiting nutrients (N, P, Fe and Si) and explicit iron cycling in the oceans with external sources from mineral dust and continental shelves (Moore et al., 2002a, 2004). The BEC model simulates the oceanic cycles of C, N, P, Si, O and Fe, and predicts the evolution of four functional groups of phytoplankton: diatoms, diazotrophs, coccolithophores and picophytoplankton. Relative to the other phytoplankton groups, the diazotrophs have higher iron and light requirements, slower maximum growth rates, and an N/P ratio of 50 (mol/mol) well above the Redfield value used for the other biota. Thus, as dust deposition varies, the model is able to capture the shifts in community composition and biogeochemical rates observed in the HNLC iron-fertilization experiments and similar ecosystem changes in low-latitude regimes where significant nitrogen fixation is observed (Moore et al., 2004). The BEC is one of several recently developed so-called dynamic green ocean models (DGOMs) specifically designed to study climate-biota feedbacks (Le Quéré et al., 2005).

The ecosystem module is coupled with a carbon cycle biogeochemistry module derived originally from the Ocean Carbon Model Intercomparison Project (OCMIP; Doney et al., 2004) and a particle sinking/remineralization parametrization following the ballast model of Armstrong et al. (2002). A full prognostic iron cycle is incorporated, and oceanic iron concentrations are governed by atmospheric and continental shelf sources, physical circulation, biological production and scavenging sinks, and subsurface remineralization (Moore et al., 2002a, 2004). The iron scavenging timescale depends upon dissolved iron and particle concentrations and can vary from a few months to a few years in surface waters. The BEC model reproduces observed global-scale patterns of primary and export production, biogenic silica production, calcification and nitrogen fixation for the current era (Moore et al., 2002b, 2004).

Most parameter values and biological initial conditions for the BEC ocean model are the same as in Moore et al. (2004). In our description here, we focus on differences in model implementation from that work. Several of the parameter values concerning iron cycling were modified with the net effect of increasing scavenging (lowering dissolved iron concentrations) in the deep ocean while maintaining similar rates (and iron concentrations) in the upper ocean. These changes bring the model into better agreement with the sparse observations of deep ocean iron concentrations, which were often too high using the Moore et al. (2004) parameter values (approaching 0.6 nM throughout the deep ocean). There were some additional changes that marginally improved simulation results. A lower temperature scaling Q10 value was used for the remineralization of soft particulate organic matter (POM), and a higher Q10 value for the remineralization of sinking biogenic silica was employed. A Q10 value of 2.0 was maintained within the ecosystem model. All parameter changes are summarized in Table 1

Table 1. Parameter changes modified in this work relative to Moore et al. (2004)

Parameter	Original value	Modified value	Units
Ref˙Particle	0.0066	0.0023	nmolC/cm^2/s[a]
Fe˙max˙scale	4.0	3.0	Unitless[b]
Fe˙scav˙threshold	0.4	0.5	NM Fe[c]
POC˙fescav˙scale	0.002	0.0002	Unitless[d]
Diatom Kfe	0.16	0.15	NM Fe[e]
CaCO3˙temp	5.0	2.0	^{o}C
alphaChl	0.25	0.28	nmolC/cm^2/ngChlWday[g]
alphaDiaz	0.03	0.036	nmolC/cm^2/ngChlWday[f]
diatom Knh4	0.008	0.1	MM N
Diazotroph Kpo4	0.0075	0.005	MM P
Diazotroph Kfe	0.1	0.09	NM Fe
Diazotroph max Fe/C	48.0	38.0	μmolFe/molC
Diazotroph P/C ratio	45.0	50.0	MolP/molC
Diazotroph mortality	0.18	0.16	Per day
Soft POM remin	42.0	115.0	m[g]
Q10 soft POM	2.0	1.25	Unitless
Soft bSi remin	32.0	55.0	m[h]
Q10 soft bSi	2.0	3.5	Unitless
Hard fraction bSi	0.55	0.1	Unitless[i]

[a]Reference particle flux used in calculating iron scavenging rates.
[b]Unitless maximum scaling factor of scavenging dependent on sinking particle flux.
[c]Threshold value below which iron scavenging rates are progressively decreased.
[d]Scaling factor for standing stock of particulate organic carbon used in Fe scavenging.
[e]Half saturation value for iron uptake by the diatoms.
[f]Initial slope of P versus I curve.
[g]Remineralization length scale for soft particulate organic matter.
[h]Remineralization length scale for soft biogenic silica.
[i]Fraction of bSi resistant to dissolution within water column.

(for additional BEC model details see Moore et al., 2002a, 2004). The current model also includes a parameterization of water column denitrification. Imbalances between nitrogen fixation and denitrification can impact ocean N inventory and associated biogeochemical cycling over centennial timescales, but have relatively little impact over the decadal timescales examined here.

To initialize our control case, the ocean model was forced with the Current dust deposition for 160 yr beginning with climatological temperature, salinity, and nutrient distributions (Conkright et al., 1998) and pre-industrial ocean inorganic carbon and alkalinity distributions (Key et al., 2004). The ocean was then integrated for an additional 40 yr with each of the four dust deposition estimates. The only forcing that varied between these simulations was dust deposition. Winds and other physical climate forcings were from a late 20th century, repeat annual cycle climatology based on the NCAR-NCEP reanalysis data set (Large and Yeager, 2004). Atmospheric CO_2 concentrations were set everywhere at pre-industrial levels (278 ppm) for all simulations. These experiments are not comprehensive climate projections, but rather a test of ocean biogeochemical sensitivity to a step function change in dust deposition that allows us to examine the influence of dust deposition as a distinct forcing separate from other climate factors that modify temperature, circulation, and stratification.

3. Results

Relative to the Current era control, the Pre-industrial and LGM dust deposition simulations increase the total dust flux to the oceans by factors of 1.6 and 4.2, respectively, while the Future simulation results in a 63% decrease in ocean dust deposition, with much of the decrease located in the Southern Hemisphere (Fig. 1). These results are similar to those obtained previously (Mahowald et al., 1999; Mahowald and Luo, 2003). The LGM increase in deposition is greater than 10-fold at high southern latitudes, similar to values seen in ice cores (e.g. Petit et al., 1990). The strong decrease in dust deposition in the Future simulation is driven by changes in winds, precipitation, soil moisture patterns, and expanded plant cover due to CO_2 fertilization.

In the final 40 yr of the Current climate simulation, nitrogen fixation, sinking particulate export production and air–sea CO_2

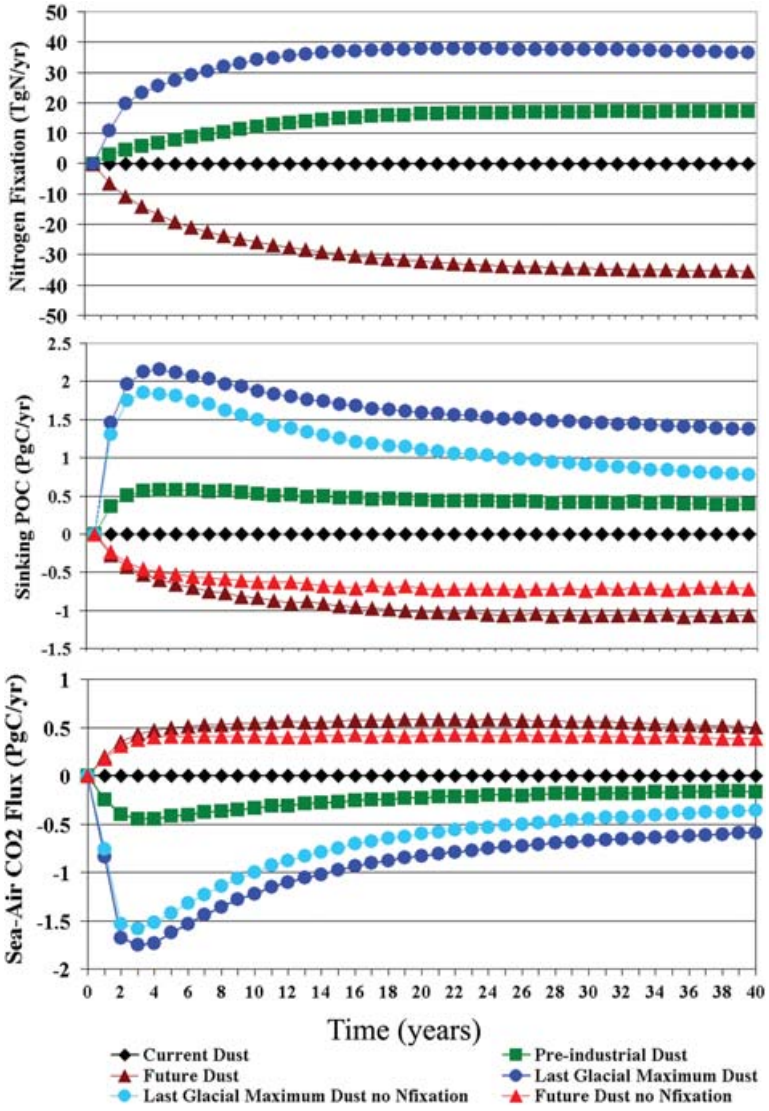

Fig. 2. Time-series of key ocean biogeochemical fluxes are shown as differences from the Current era dust control simulation. For the Future and Last Glacial Maximum simulations, results are shown with and without nitrogen fixation, in each case relative to the corresponding Current era dust control.

flux were steady at 75 TgN/yr, 5.5 PgC/yr, and 0.24 PgC/yr net ocean uptake. The small net CO_2 uptake reflects slow subsurface drift and the long timescales, order thousands of years, required for the ocean inorganic carbon system to reach full-equilibrium (Doney et al., 2004). The drift in each of these fluxes over the last 40 yr of this control simulation were -1.5% for nitrogen fixation, -0.11% for sinking export and -5.2% for net sea-air CO_2 flux. These drifts are quite small compared with the differences between our simulations. Similarly small drifts were seen in a sensitivity experiment with a Current dust control simulation without an active nitrogen cycle (see below). Our simulated nitrogen fixation rates are on the low end of recent observational estimates, which typically exceed 100 TgN/yr (Karl et al., 2002; Galloway et al., 2004; Gruber, 2004).

In the analysis below, net global air–sea CO_2 and biogeochemical fluxes are reported as differences from this Current dust simulation to highlight the impact of the dust perturbations. In Fig. 2, we plot time-series of the differences in global biogeochemical rates from the Current dust control simulation for each alternate dust deposition, following the step-change perturbation. Under the Pre-industrial and LGM dust deposition scenarios, there were large increases in nitrogen fixation, sinking particulate organic carbon (POC) export, and ocean uptake of atmospheric CO_2. Sinking POC export at 103 m initially increased by more than 2 PgC/yr ($+36\%$) under the dustier LGM conditions, driving an increase in the uptake of CO_2 from the atmosphere of more than 1.5 PgC/yr. The difference in CO_2 uptake between the Current and LGM simulations declined over the simulation but was still $\sim$0.6 PgC/yr after 40 yr. The decreases in dust deposition in the Future climate simulation led to greatly reduced rates of nitrogen fixation (-45%) and export production (-20%), driving net out-gassing of $\sim$0.5 PgC/yr of CO_2 (Fig. 2). Note that all our

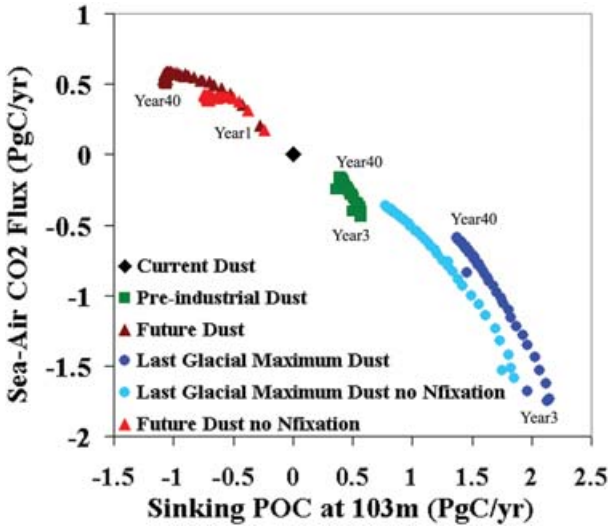

Fig. 3. Sea-air CO2 flux is plotted versus sinking particulate organic carbon export (POC) relative to Current era dust control simulations for each dust-forcing scenario. For the Future and Last Glacial Maximum simulations, results are shown with and without nitrogen fixation, in each case relative to the corresponding Current era dust control.

simulations use a constant pre-industrial atmospheric CO_2 value; at current or future atmospheric CO_2 values this 'out-gassing' would be expressed as reduced ocean uptake.

The strong influence of biological carbon export out of surface waters (the biological pump) on air–sea CO_2 flux is apparent if we plot annual export production versus air–sea CO_2 flux from each year of the four simulations, again as differences from our control simulations (Fig. 3). We have marked years 3 (maximum perturbation in air–sea CO_2 exchange) and 40 in Fig. 3 to highlight the early response and drift over the simulation for the LGM and Pre-industrial simulations (and similarly years 1 and 40 for the Future dust case). The net ocean uptake increases with export production with a linear fit slope to the data points from our four main simulations of -0.59 (with $r^2 = 0.96$), indicating an ocean CO_2 uptake of approximately 0.6 PgC for every 1 PgC exported below 103 m. This slope declines to -0.45 if only the last simulation year from the four simulations are considered. These results highlight the importance of the biological pump in controlling air–sea CO_2 exchange, with more export leading to lower surface pCO_2 values and increased uptake of atmospheric CO_2, and the opposite effect where export production declines. These results also illustrate how iron inputs from the atmosphere can decouple production, export and net air–sea CO_2 flux from the physical processes driving macronutrient and dissolved inorganic carbon inputs from subsurface waters, in a manner similar to the decoupling due to new nitrogen inputs from nitrogen fixation (Michaels et al., 2001). In a simulation with constant dust deposition and a simpler ocean biogeochemical model than used here, Doney et al. (2006) actually found a negative correlation between export and ocean CO_2 uptake. Since export production was driven mainly by nutrient entrainment from subsurface waters, years with higher export also had higher DIC concentrations in surface waters and thus anomalous CO_2 out-gassing.

To examine the relative impact of the direct versus indirect iron pathways on the ocean carbon cycle, we conducted additional sensitivity simulations with nitrogen fixation and denitrification set equal to zero for Current dust forcing (200 yr simulation) and with Future and LGM dust depositions (40 yr simulation, again branching from the corresponding Current dust control simulation after year 160). The Future and LGM results with and without nitrogen fixation and denitrification are shown in Figs. 2 and 3 relative to their respective Current dust control simulations. The short-term response to increased dust deposition is dominated by the direct pathway; when dust deposition is increased to the LGM levels, the direct pathway, initially accounts for 89% of the change in export production and 91% of the change in air–sea CO_2 flux. However, the relative importance of the indirect pathway increases with time, accounting for 46% of the total change in export production and 38% of the total change in air–sea CO_2 flux in the LGM dust simulation relative to the control in year 40. A similar pattern was seen in the response to the reduced Future dust deposition, with the initial 88% reduction in export and 86% reduction in ocean uptake of CO_2 due to the direct pathway declining to 67% and 76%, respectively, by year 40. Thus, over shorter timescales of less than a decade, the direct pathway dominates the ocean biogeochemical response to changes in dust deposition; but over decadal and longer timescales the indirect pathway may be equally important.

The timescales of ocean biogeochemical response depend on the sign of the dust deposition perturbation and on modifications of the direct and indirect pathways. In the Pre-industrial and LGM dust deposition perturbation simulations, there is a rapid ($\sim$5 yr) increase in export of POC and ocean uptake of CO_2 (Fig. 2). The subsequent decline in the POC export and ocean CO_2 uptake anomalies occurs as nutrients other than iron become limiting for phytoplankton growth in some HNLC regions. Note, however, that under the elevated Pre-industrial and LGM dust deposition the ocean biogeochemical rates approach new steady-state values that differ significantly from the Current dust control. These results imply that the oceans can respond relatively quickly to a sharp increase in dust deposition even over interannual timescales and that there are longer-term adjustments in ocean nutrient reservoirs and biogeochemical dynamics. In contrast, in the Future dust simulation the decrease in export production and ocean CO_2 uptake occurs more gradually as subsurface iron pools are depleted, taking about two decades to approach a new quasi-steady state (Fig. 2). The residence time for dissolved iron in the upper ocean is likely only a few years to a decade (de Baar and de Jong, 2001; Moore et al., 2004). Similarly, the response of nitrogen fixation to changes in dust deposition is also more gradual, taking nearly three decades before stabilizing (Fig. 2). The diazotrophs are responding to changes in the subsurface iron concentrations advected from

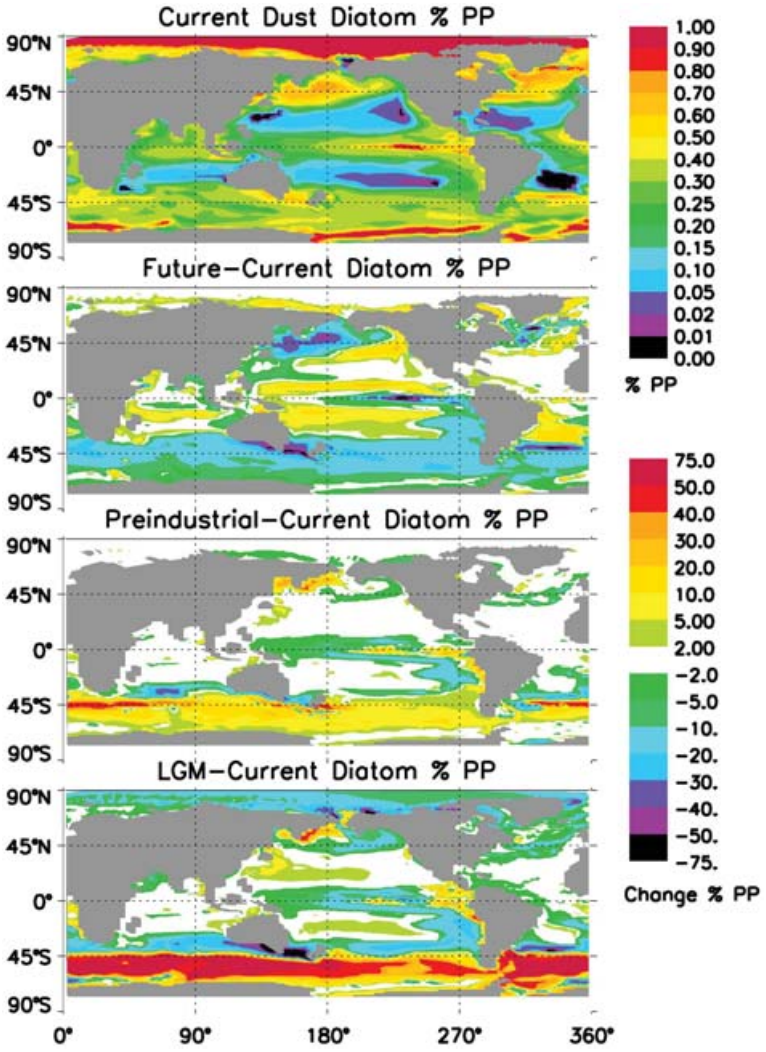

Fig. 4. The percentage of total primary production by diatoms in our Current era dust control simulation is shown along with the change in diatom percentage contribution in each of the other simulations relative to the Current era dust control.

regions with large changes in dust deposition. In a given year, some 70–80% of the iron utilized by phytoplankton comes from subsurface sources (Moore et al., 2002b, 2004; Aumont et al., 2003).

These changes in ocean biogeochemical cycling and air–sea CO_2 exchange are driven by changes in the phytoplankton community composition and in the degree of nutrient stress. Under the Pre-industrial and LGM dust forcing, diatom production and export increased dramatically fuelling increased POC export in the HNLC regions, particularly in the Southern Ocean (Figs. 4 and 5). By the end of the simulations, the percentage of the world oceans where iron is the dominant factor limiting diatom growth rates declined from 33% with the Current dust forcing (at years 160 and 200) to 25% with Pre-industrial dust and only 13% with the LGM dust deposition. The iron-limited regions in both simulations were concentrated in the Southern Ocean, with much of the sub-Arctic and equatorial Pacific HNLC regions becoming nitrogen limited (similar patterns were seen for the small phytoplankton group). Reduced iron-stress leads to increased export and CO_2 uptake in the HNLC regions in both simulations. Under higher dust fluxes the phosphorus limited areas for the diazotrophs expand in the Atlantic and Indian oceans, and shrink under the lower Future dust deposition (shifting to iron limitation). The percentage of total primary production accounted for by the diatoms in the Pre-industrial and LGM increased dramatically in the HNLC regions, particularly in the Southern Ocean, and also increased in the subtropical gyres, particularly in the Pacific, in response to increased nitrogen fixation (Figs. 4 and 5). In general, the nutrient limitation patterns for all phytoplankton groups under the Current dust forcing are similar to our previous results (Moore et al., 2004), though with a somewhat smaller iron-limited equatorial Pacific region, and less low-latitude silicon limitation for the diatoms.

Changes in the rain ratio (sinking $CaCO_3$/sinking POC) had relatively little impact in our simulations. Typically the production of $CaCO_3$ scaled with POC export such that the global mean

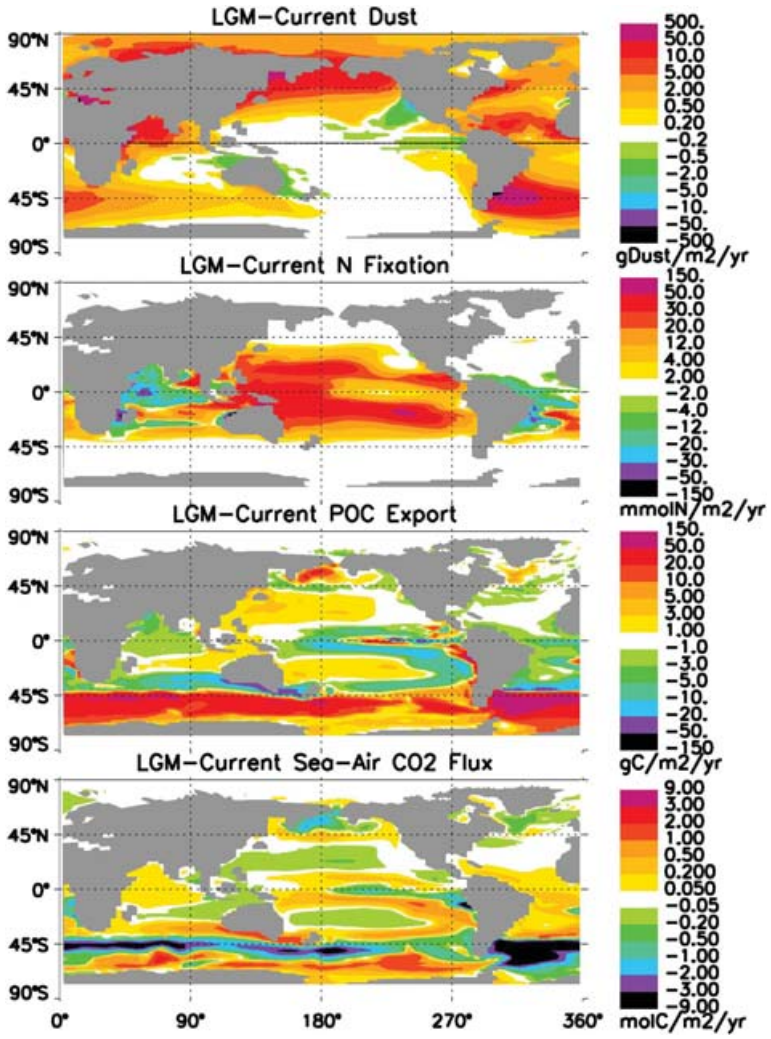

Fig. 5. The change in dust forcing and the ocean biogeochemical responses are shown for the Last Glacial Maximum (LGM) dust scenario relative to our Current era dust control. Each panel shows the difference between LGM-Current results.

rain ratio was relatively constant, despite the large variations in POC export. The global mean ratio was 0.06 (C/C) for all simulations except the LGM dust simulation, which was slightly lower at 0.05. Calcification is parametrized in the model as a variable fraction of our small phytoplankton group based on biomass, temperature and degree of nutrient stress (Moore et al., 2002a, 2004). Global calcification rates varied somewhat between the simulations with rates of 0.49 GtC/yr at the end of the control simulation, and values of 0.35, 0.50 and 0.38 GtC/yr for the LGM, Pre-industrial and Future dust simulations, respectively. Calcification was lower with the LGM dust due to a community shift towards increased diatom production, and lower with the Future dust due to increased nutrient stress on the smaller phytoplankton.

Mineral dust particles play important roles in the BEC model. They serve as a key source of dissolved iron to the oceans (and as a source of particles that scavenge iron), and they act as mineral ballast (Armstrong et al., 2002) influencing the flux of POM to the deep ocean. To examine the relative impact of these two roles in our simulations, we conducted two additional sensitivity simulations, one where dust flux was held constant but dissolved iron release was doubled relative to our control, and a second simulation where dust flux was doubled but dissolved iron release was held constant (Table 2). Biogeochemical fluxes in the doubled-dust simulation were nearly identical to our control, and the doubled-iron simulation had large increases in export, nitrogen fixation, and ocean uptake of CO_2. This indicates that it is the dissolved iron release driving the results presented in this paper. This mainly reflects the fact that the mineral ballast effect is dominated by $CaCO_3$ and biogenic silica, rather than dust particles. At the end of the Current dust control simulation, for example, of the sinking POM bound to ballast (6.9% of total sinking POM) at 103m depth, 53% was bound to $CaCO_3$, 43% to biogenic silica and only 4.2% to mineral dust. The relatively short timescale of our simulations also plays a role, as the altered flux of organic matter to the deep ocean would become more important over longer timescales.

Table 2. Sensitivity simulations designed to separate the two roles played by dust in the model as a source for dissolved iron and as a mineral ballast. Our control simulation (current era dust) is compared with 40 yr simulations where dissolved iron release was doubled but dust flux held constant (FeX2), and a simulation where dust inputs were doubled but release of dissolved iron was held constant (DustX2). Selected biogeochemical fluxes for each simulation are shown (primary production (GtC/yr), sinking POC flux at 103m (GtC/yr), sinking dust particle flux at 103m (Gt/yr), nitrogen fixation (TgN/yr) and the percentage of primary production by diatoms).

	PrimaryP	SinkPOC	SinkDust	Nfixation	%Diatoms
Control	44.8	5.51	0.23	76.3	33.4
DustX2	44.7	5.49	0.46	75.8	33.4
FeX2	46.1	5.96	0.23	103.7	36.5

The spatial patterns associated with the LGM dust deposition and the ocean biogeochemical response to this forcing, relative to the Current dust control, are highlighted in Fig. 5. Large increases in dust deposition at high latitudes drive increased POC export and oceanic uptake of atmospheric CO_2, particularly in the North Pacific and mid-latitude Southern Ocean. In the Southern Ocean, the largest dust increases are in the Atlantic sector, with moderate increases in the Indian sector, and no large increase in Pacific dust forcing. The ocean perturbation follows this pattern with the largest export increase in the Atlantic sector progressively decreasing downstream, consistent with results from sediment core analysis (Chase et al., 2003; Kohfeld et al., 2005). Increased nitrogen fixation in the Pacific basin and South Indian subtropical gyres drives smaller increases in POC export and CO_2 uptake (Fig. 5). Other low-latitude regions downstream of the Southern Ocean exhibit decreased productivity because of lower lateral transport of preformed macronutrients that are stripped from surface source waters in the Sub-Antarctic mode and Antarctic Intermediate water formations sites (results similar to Sarmiento et al., 2004b). Nitrogen fixation does not increase in the northern Atlantic and Indian basins despite increased dust deposition because the diazotrophs are largely phosphorus limited in these regions. Spatial patterns for the Pre-industrial dust deposition relative to the control were very similar, but flux changes were smaller in magnitude.

The spatial patterns of projected decreased dust deposition and the ocean biogeochemical response for the Future case are shown in Fig. 6, again relative to the Current control. Dust deposition decreases globally with the largest decreases in the Arabian Sea and near the major source regions in Asia, Africa, Australia, and South America. In response, POC export decreases and ocean CO_2 out-gassing increases in each of the HNLC regions. Note that in contrast to the LGM, the strongest POC and air–sea flux signals occur on the northern edge or north of the simulated Antarctic Circumpolar Current. Nitrogen fixation declines sharply in the Pacific and South Indian basins, leading to increased sea to air CO_2 flux relative to the Current era control (Fig. 6). Nitrogen fixation increases along South America and in the eastern Arabian Sea, driving increased export and CO_2 uptake in those regions. This pattern in both regions is due to reduced phosphorus stress for the diazotrophs, due to less phosphate utilization by the other phytoplankton groups, locally and in upstream regions. Diatom and diazotroph production and biomass were both reduced significantly under the Future dust forcing, with the community shifted toward the smaller picophytoplankton. The global area where iron limits diatom growth increased to 59%, including the entire South Pacific and a general expansion of the HNLC zones. The results from these alternate dust deposition scenarios are qualitatively similar to our previous results where the Current era dust deposition was simply increased or decreased everywhere by constant factors (Moore et al., 2002b, 2004).

4. Discussion

Across all the simulations, the most dramatic differences in biogeochemical fluxes were seen in the HNLC areas in response to the direct iron pathway; however, significant differences in export production and air–sea CO_2 flux also occurred within the subtropical gyres in response to the indirect nitrogen fixation pathway (Figs. 4–6). Even small changes in areal export production and air–sea CO_2 flux in these regions can have a global impact, as they account for a large fraction of open ocean area (Martin et al., 1987). These results highlight the role of the nitrogen fixers in amplifying the ocean biogeochemical response to variations in dust deposition, particularly over decadal timescales (Fig. 2).

Our results have implications for predicting climate change over the next century and for understanding past climate regimes. If the simulated decreases in mineral dust deposition do occur over the 21st century, oceanic uptake of anthropogenic CO_2 will be significantly reduced due to ecosystem and biogeochemical changes along both the direct and indirect pathways. This would provide a positive feedback to the ongoing global warming (Michaels et al., 2001) in addition to feedbacks associated with increased ocean stratification and circulation changes (Sarmiento et al., 1994a, 1998; Bopp et al., 2001; Friedlingstein et al., 2003; Fung et al., 2005). The changes in export and air–sea CO_2 flux in this study are similar in magnitude to estimates of these other ocean CO_2-climate feedbacks, ranging from $\sim$0.5 to 1.5 PgC/yr (Sarmiento et al., 1998; Bopp et al., 2001). Our simulations suggest that decreasing dust inputs from the Pre-industrial to the present could have already resulted in a sustained reduction in ocean CO_2 uptake of $\sim$0.2 PgC/yr, a significant fraction of current estimates of net ocean uptake of $\sim$2 PgC/yr (Le Quéré et al., 2003). The decreased ocean uptake of CO_2 between the Pre-industrial and Current dust simulations are concentrated in the HNLC regions and the south Pacific subtropical gyre. The

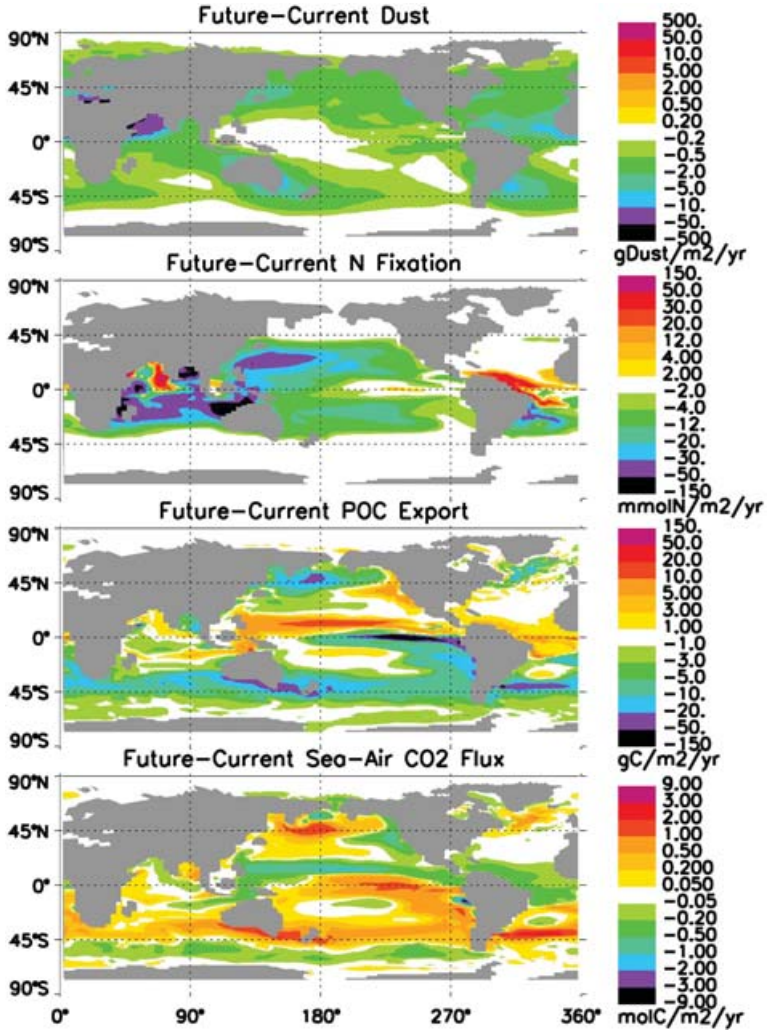

Fig. 6. The change in dust forcing and the ocean biogeochemical responses are shown for the Future dust scenario relative to our Current era dust control. Each panel shows the difference between Future-Current results.

dust effect on net CO_2 uptake in the simulations increases to ~0.7 PgC/yr out-gassing by 2100 relative to pre-industrial conditions (Future minus Pre-industrial simulations). The atmospheric dust deposition scenarios used here are for equilibrium conditions to the new climate/CO_2 states, neglecting the finite response timescales for changes in terrestrial vegetation and dust sources. In order to directly relate to ocean field observations, further work is required to define the transient climate/CO_2 response of land dust sources. In some cases dust forcing may work in the opposite direction of other climate feedbacks. Increased stratification over the next century, for example, could act to increase nitrogen fixation rates (Hansell and Feely, 2000; Boyd and Doney, 2002).

A recent glacial maximum simulation found a reduction in atmospheric CO_2 of ~15 ppm due to higher dust fluxes driving increased export production along the direct pathway (Bopp et al., 2003), but these results did not include the indirect pathway for dust to influence the ocean carbon cycle via nitrogen fixation. Small increases in export production in the subtropical gyres during glacial periods could significantly impact atmospheric CO_2 levels but would be difficult to detect in sediment cores from these low-flux regions. While the transient, multidecade simulations here are insufficient to quantify the longer-term oceanic response to glacial conditions, they do suggest a role for the indirect nitrogen fixation pathway in the glacial lowering of atmospheric pCO_2 (Falkowski, 1997).

Our simulations illustrate that there is a significant decadal timescale response of ocean biogeochemistry to variations in mineral dust deposition. Over centennial and longer timescales, there would be additional feedbacks as subsurface nutrient concentrations were modified and advected, influencing downstream regions (Sarmiento et al., 2004b). Dust deposition for the current climate and the LGM are moderately constrained by observational data (Luo et al., 2003; Mahowald et al., 1999, 2006). Palaeo-records of dust are used to constrain the LGM deposition for these simulations (Kohfeld and Harrison, 2001; Mahowald et al., 2006). However, there is considerable uncertainty with our estimates of the change in dust deposition from the pre-industrial to present, as well as into the future. Not included in these

simulations are changes in dust emissions to the atmosphere due to human land use activities, which might increase dust fluxes by anywhere from 0–50% (Mahowald et al., 2004; Tegen et al., 2004). Expansion of agriculture in arid regions could act to reduce dust emissions. The centennial timescale response of vegetation on the continents to rising atmospheric CO_2 levels adds additional uncertainty.

There is a critical need for increased global monitoring and process level understanding of mineral dust sources, transport and deposition, surface ocean trace metal concentrations, and ocean ecosystem dynamics. These studies are necessary to understand the climate feedbacks outlined here, better constrain ocean biogeochemical models, and to accurately predict future climate change. From a marine ecological perspective, specific research needs to include better quantitative estimates of the response of surface water and upper ocean iron concentrations, export and community structure to natural dust perturbations (as opposed to large artificial perturbation experiments). Atmospheric dust deposition undergoes substantial temporal variations on synoptic to interannual timescales, a fact that could be exploited in the development of targeted field experiments.

5. Acknowledgements

This work was supported by grants from the U.S. National Science Foundation (OCE-0323332, OCE-0222033, OCE-9981398 and OCE-0452972) and from the National Aeronautics and Space Administration (NAG5-9671). Computations supported by Earth System Modeling Facility (NSF ATM-0321380) and by the Climate Simulation Laboratory at the National Center for Atmospheric Research. The National Center for Atmospheric Research is sponsored by the U.S. National Science Foundation. The authors thank Nick Stephens and an anonymous reviewer for helpful comments.

References

Armstrong, R. A., Lee, C. Hedges, J. I., Honjo, S. and Wakeham, S. G. 2002. A new, mechanistic model for organic carbon fluxes in the ocean based on the quantitative association of POC with ballast minerals. *Deep-Sea Res.* Part II **49**, 219–236.

Aumont, O., Maier-Reimer, E., Blain, S. and Monfray, P. 2003. An ecosystem model ofthe global ocean including Fe, Si, P co-limitations. *Global Biogeochem. Cycles* **17**, 1060, doi:10.1029/2001GB001745.

Berman-Frank, I., Cullen, J. T., Shaked, Y., Sherrell, R. M. and Falkowski, P. G. 2001. Iron availability, cellular iron quotas, and nitrogen fixation in *Trichodesmium*.*Limnol. Oceanogr.* **46**, 1249–1260.

Bopp, L., Kolfield, K. E., Le Quérê, C. 2003. Dust impact or morine b:oto and atmospheric CO_2 during glacid periods. Paleoceanography. lp(2),1046. doi: 11029/2002PA000810.

Bopp, L., Monfray, P., Aumont, O., Dufresne, J. L., Treut, H. L. and co-authors. 2001. Potential impact of climate change on marine export production. *Global Biogeochem. Cycles* **15**, 81–99.

Boyd, P. W., Watson, A. J., Law, C. S., Abraham, E. R., Trull, T. and co-authors. 2000.Phytoplankton bloom upon mesoscale iron fertilization of polarsouthernocean waters. *Nature* **407**, 695–702.

Boyd, P. W. and Doney, S. C. 2002. Modelling regional responses by marine pelagic ecosystems to global climate change. *Geophys. Res. Lett.* **29**(16), 53-1–53-4, doi:10.1029/2001GL014130.

Chase, Z., Anderson, R. F., Fleisher, M. Q. and Kubik, P. W. 2003. Accumulation of biogenic and lithogenic material in the Pacific sector of the Southern Ocean during the past 40,000 years. *Deep-Sea Res. II* **50**, 799–832.

Coale, K. H., Johnson, K. S., Fitzwater, S. E., Gordon, R. M., Tanner, S. and co-authors. 1996. Amassive phytoplankton bloom induced by an ecosystem-scale iron fertilizationexperiment in the equatorial Pacific Ocean. *Nature* **383**, 495–501.

Coale, K. H., Johnson, K. S., Chavez, F. P., Buesseler, K. O., Barber, R. T. and co-authors. 2004. Southern Ocean Iron Enrichment Experiment: carbon cycling in high- and low-Siwaters. *Science* **304**, 408–414.

Collins, W. D., Blackmon, M., Bitz, C. M., Bonan, G. B., Bretherton, C. S. and co-authors. 2006. The Community Climate System Model: CCSM3. *J. Climate* **19**, 2122–2143.

Conkright, M. E., Levitus, S., O'Brien, T., Boyer, T. P. Stephens, C. and co-authors. 1998. World Ocean Database 1998 CD-ROM data set documentation, Internal Rep. 14, Natl. Oceanogr. Data Cent., Silver Spring, MD.

de Baar, H. J. W., Boyd, P. W., Coale, K. H., Landry, M. R., Tsuda, A. and co-authors. 2005. Synthesis of 8 iron fertilization experiments: from the Iron Age in the Age of Enlightenment. *J. Geophys. Res.* **110**, C09S16, doi:10.1029/2004JC002601.

de Baar, H. J. W. and De Jong, J. T. M. 2001. Distributions, sources and sinks of iron in seawater. In: *Biogeochemistry of Iron in Seawater* (eds.D. Turner and K. A. Hunter). IUPAC Book Series on Analytical and Physical Chemistry of Environmental Systems **7**, 123–253.

Doney, S. C., Lindsay, K., Fung, I. and John, J. 2006. Natural variability in a stable 1000 year coupled climate-carbon cycle simulation. *J. Climate* **19**, 3033–3054.

Doney, S. C., Lindsay, K., Caldeira, K., Campin, J. M., Drange, H. and others 2004. Evaluating global ocean carbon models: the importance of realistic physics. *Global Biogeochem. Cycles* **18**, GB3017, doi:10.1029/2003GB002150.

Falkowski, P. G. 1997. Evolution of the nitrogen cycle and its influence on the biological sequestration of CO2 in the ocean. *Nature* **387**, 272–275.

Friedlingstein, P., Dufresne, J. L., Cox, P. M. and Rayner, P. 2003. How positive is thefeedback between climate change and the carbon cycle? *Tellus* **55B**, 692–700.

Fung, I., Doney, S. C., Lindsay, K. and John, J. 2005. Evolution of carbon sinks in a changing climate. *Proc. Nat. Acad. Sci. (USA)* **102**, 11201–11206, doi:10.1073/pnas.0504949102.

Fung, I. Y., Meyn, S. K., Tegen, I., Doney, S. C., John, J. G. and co-authors. 2000. Iron supply and demand in the upper ocean. *Global Biogeochem. Cycles* **14**, 281–295.

Galloway, J. N., Dertener, F. J. Capone, P. G., Boyer, E. W., Howarth, R. W. and co-authors. 2004. Nitrogen Cycles: past, present and future. *Biogeodemistry* **70**, 153–226.

Glibert, P. M. and Bronk, D. A. 1994. Release of dissolved organic nitrogen by marine diazotrophic cyanobacteria, *Trichodesmium* spp. *Appl. Environ. Microbiol.* **60**, 3996–4000.

Grini, A. and Zender, C. 2004. Roles of saltation, sandblasting, and wind speed variability on mineral dust aerosol size distribution during the Puerto Rican Dust Experiment (PRIDE). *Journal of Geophysical Research* **109**(D7), D07202, doi:10.1029/2003JD004233.

Gruber, N. 2004. The dynamics of the marine nitrogen cycle and its influence on atmospheric CO_2 variations. In: *The Ocean Carbon Cycle* (eds. Follows, M. and Oguz, T.) Kluwer Academic Publishers, Netherlands, pp. 97–148.

Hansell, D. A. and Feely, R. A. 2000. Atmospheric intertropical convergence impacts surface ocean carbon and nitrogen biogeochemistry in the western tropical Pacific. *Geophysical Res. Lett.* **27**, 1013–1016.

Haxeltine, A. and Prentice, I. C. 1996. BIOME3: an equilibrium terrestrial biosphere model based on ecophysiological constraints, resource availability, and competition among plant functional types. *Global Biogeochem. Cycles* **10**(4), 693–709.

Jickells, T. D., An, Z. S., Anderson, K. K., Baker, A. R., Bergametti, G. and co-authors. 2005. Global iron connections between desert dust, ocean biogeochemistry, and climate, *Science* **308**, 67–71.

Karl, D., Michaels, A., Bergman, B., Capone, D., Carpenter, E. and co-authors. 2002. Dinitrogen fixation in the world's oceans. *Biogeochemistry* **57/58**, 47–98.

Key, R. M., Kozyr, A., Sabine, C. L., Lee, K., Wanninkhof, R. and co-authors. 2004. A global ocean carbon climatology: results from Global Data Analysis Project (GLODAP). *Global Biogeochem. Cycles* **18**, GB4031, doi:10.1029/2004GB002247.

Kiehl, J. T., Shields, C. A., Hack, J. J. and Collins, W. 2006. The climate sensitivity of the Community Climate System Model: CCSM3. *J. Climate* **17**, 2584–2596.

Kohfeld, K. E. and Harrison, S. P. 2001. DIRTMAP: the geological record of dust. *Earth Sci. Rev.* **54**, 81–114.

Kohfeld, K. E., Le Quéré, C., Harrison, S. P. and Anderson, R. F. 2005. Role of marine biology in glacial-interglacial CO2 cycles. *Science* **308**, 74–78.

Kustka, A., Carpenter, E. J. and Sañudo-Wilhelmy, S. 2002. Iron and marine nitrogen fixation: progress and future directions. *Res. Microbiology* **153**, 255–262.

Kustka, A., Sañudo-Wilhelmy, S., Carpenter, E. J., Capone, D. G. and Raven, J. A. 2003. A revised estimate of the iron use efficiency of nitrogen fixation, with special reference to the marine cyanobacterium *Trichodesmium SPP*. (CYANOPHYTA). *J. Phycol.* **39**, 12–25.

Large, W. G. and Yeager, S. G. 2004. Diurnal to decadal global forcing for ocean and sea-ice models: the data sets and flux climatologies. *NCAR Technical Note NCAR/TN-460+STR*, 111 pp.

Le Quéré, C., Aumont, O., Bopp, L., Bousquet, P., Ciaes, P. and co-authors. 2003. Two decades of ocean CO_2 sink and variability *Tellus* **55B**, 647–656.

Le Quéré, C., Harrison, S. P., Prentice, I. C., Buitenhuis, E. T., Aumont, O. and co-authors. 2005. Ecosystem dynamics based on plankton functional types for global ocean biogeochemistry models, *Global Change Biol.* **11**, 2016–2040.

Luo, C., Mahowald, N. and del Corral, J. 2003. Sensitivity study of meteorological parameters on mineral aerosol mobilization, transport and distribution. *J. Geophys. Res.* **108**(D15), 4447, 10.1029/2003JD0003483.

Mahaffey, C., Michaels, A. F. and Capone, D. G. 2005. The Conundrum of marine N_2 fixation. *Amer. J. Sci.* **305**, 546–595.

Mahowald, N. M. and Luo, C. 2003. A less dusty future? *Geophys. Res. Lett.* **30**(17), 1903, doi:10.1029/2003GRL017880.

Mahowald, N., Kohfeld, K., Hansson, M., Balkanski, Y., Harrison, S. P. and co-authors. 1999. Dust sources and deposition during the last glacial maximum and current climate: a comparison of model results with paleodata from ice cores and marine sediments. *Journal of Geophysical Research* **104**(D13), 15 895–15 916.

Mahowald, N., Rivera, G. and Luo, C. 2004. Comment on "Relative importance of climate and land use in determining present and future global soil dust emission" (ed.I. Tegen et al.), *Geophys. Res. Lett.* **31**(24), L24105, doi:10.1029/2004GL021272.

Mahowald, N. M., Baker, A. R., Bergametti, G., Brooks, N., Duce, A. and co-authors. 2005. Atmospheric global dust cycle and iron inputs to the ocean. *Global Biogeochem. Cycles* **19**, GB4025, doi:10.1029/2004GB002402.

Mahowald, N. M., Muhs, D. R., Levis, S., Rasch, P. J, Yoshioka, M. and co-authors. 2006. Change in atmospheric mineral aerosols in response to climate: last glacial period, preindustrial, modern, and doubled carbon dioxide climates *J. Geophys. Res.* **111**, D10202, doi:10.1029/2005JD006653.

Martin, J. H., Knauer, G. A., Karl, D. M. and Broenkow, W. W. 1987. VERTEX: carbon cycling in the northeast Pacific. *Deep-Sea Res.* **34**, 267–285.

Martin, J. H., Gordon, R. M., Fitzwater, S. E. 1991. The case for iron. *Limnol. Oceanogr.* **36**, 1793–1802.

Michaels, A. F., Karl, D. M. and Capone, D. G. 2001. Elemental stoichiometry, new production, and nitrogen fixation. *Oceanography* **14**(4), 68–77.

Moore, J. K., Doney, S. C., Kleypas, J. C., Glover,D. M. and Fung, I. Y. 2002a. An intermediate complexity marine ecosystem model for the global domain. *Deep-Sea Res. II* **49**, 403–462.

Moore, J. K., Doney, S. C., Glover, D. M. and Fung, I. Y. 2002b. Iron cycling and nutrient limitation patterns in surface waters of the world ocean *Deep-Sea Res. II* **49**, 463–508.

Moore, J. K., Doney, S. C. and Lindsay, K. 2004. Upper ocean ecosystem dynamics and iron cycling in a global three-dimensional model. *Global Biogeochem. Cycles* **18**, GB4028, doi:10.1029/2004GB002220.

Otto-Bliesner, B. L., Brady, E. C., Clauzet, G., Tomas, R. A., Levis, S. and co-authors. 2006. Last glacial maximum and Holocene climate in CCSM3. *J. Clim.* **17**, 2567–2583.

Petit, J. R., Mounier, L., Jouzel, J., Korotkevich, S.Y., Kotlyakov, V. I. and co-authors. 1990. Palaeoclimatological and chronological implications of the Vostok core dust record. *Nature* **343**, 56–58.

Rasch, P. J., Collins, W. and Eaton, B. E. 2001. Understanding the Indian ocean Experiment (INDOEX) aerosol distributions with an aerosol assimilation. *J. Geophys. Res.* **106**(D7), 7337–7355.

Sarmiento, J. L., Hughes, T. M. C., Stouffer, R. J. and Manabe, S. 1998. Simulated response of the ocean carbon cycle to anthropogenic climate warming *Nature* **393**, 245–249.

Sarmiento, J. L., Slater, R., Barber, R., Bopp, L., Doney, S. C. and co-authors. 2004a. Response of ocean ecosystems to climate warming. *Global Biogeochem. Cycles* **18**, GB3003, doi:10.1029/2003GB002134.

Sarmiento, J. L., Gruber, N., Brzezinski, M. A. and Dunne, J. P. 2004b. High-latitude controls of thermocline nutrients and low latitude biological productivity. *Nature* **427**, 56–60.

Tegen, I. M., Werner, M., Harrison, S. P. and Kohfeld, K. E. 2004. Relative importance of climate and land use in determining present and future global soil dust emission. *Geophys. Res. Lett.* **31**, L05105, doi:10.1029/2003GL019216.

Tsuda, A., Takeda, S., Saito, H., Nishioka, J., Nojiri, Y. and others 2003. A mesoscale iron enrichment in the western Subarctic Pacific induces a large centric diatom bloom. *Science* **300**, 958–961.

Werner, M., Tegen, I., Harrison, S., Kohfeld, K., Prentice, I. C. and co-authors. 2002. Seasonal and interannual variability of the mineral dust cycle under present and glacial climate conditions *JGR* **107**(24), 4744, doi:10.1029/2002JD002365.

Yeager, S. G., Large, W. G., Hack, J. J. and Shields, C. A. 2006. The low resolution CCSM3. *J. Climate* **17**, 2543–2566.

Zarate, M. 2003. Loess of southern South America *Quat. Sci. Rev.* **22**, 1987–2006.

Zender, C., Bian, H. and Newman, D. 2003a. Mineral Dust Entrainment and Deposition (DEAD) model: description and 1990s dust climatology. *J. Geophys. Res.* **108**(D14), 4416.

Zender, C., Newman, D. and Torres, O. 2003b. Spatial heterogeneity in aeolian erodibility: uniform, topographic, geomorphic and hydrologic hypotheses. *J. Geophys. Res.* **108**(D14), 4416, doi:10.1029/2002JD002775.